journal of the mechanical behavior of biomedical materials 125 (2022) 104872

Contents lists available at ScienceDirect

Journal of the Mechanical Behavior of Biomedical Materials

journal homepage: www.elsevier.com/locate/jmbbm

Research Paper

MicroFE models of porcine vertebrae with induced bone focal lesions: Validation of predicted displacements with digital volume correlation

Marco Palanca *, Sara Oliviero, Enrico Dall'Ara

Dept of Oncology and Metabolism, And INSIGNEO Institute for in silico medicine, University of Sheffield, Sheffield, UK

ARTICLE INFO

Keywords:
Induced lesions
Vertebra
Spine
Validation
Micro finite element model
Digital volume correlation

ABSTRACT

The evaluation of the local mechanical behavior as a result of metastatic lesions is fundamental for the characterization of the mechanical competence of metastatic vertebrae. Micro finite element (microFE) models have the potential of addressing this challenge through laboratory studies but their predictions of local deformation due to the complexity of the bone structure compromized by the lesion must be validated against experiments. In this study, the displacements predicted by homogeneous, linear and isotropic microFE models of vertebrae were validated against experimental Digital Volume Correlation (DVC) measurements. Porcine spine segments, with and without mechanically induced focal lesions, were tested in compression within a micro computed tomography (microCT) scanner. The displacement within the bone were measured with an optimized global DVC approach (BoneDVC). MicroFE models of the intact and lesioned vertebrae, including or excluding the growth plates, were developed from the microCT images. The microFE and DVC boundary conditions were matched. The displacements measured by the DVC and predicted by the microFE along each Cartesian direction were compared. The results showed an excellent agreement between the measured and predicted displacements, both for intact and metastatic vertebrae, in the middle of the vertebra, in those cases where the structure was not loaded beyond yield ($0.69 < R^2 < 1.00$). Models with growth plates showed the worst correlations ($0.02 < R^2 < 0.99$), while a clear improvement was observed if the growth plates were excluded ($0.56 < R^2 < 1.00$). In conclusion, these simplified models can predict complex displacement fields in the elastic regime with high reliability, more complex non-linear models should be implemented to predict regions with high deformation, when the bone is loaded beyond yield.

1. Introduction

Bone metastatic lesions most frequently occur in the spine. These lesions may lead to spine instability (Roodman, 2004) in addition to the other related complications (Laufer et al., 2013). The high variability in the type, size, and position of the metastasis affects the mechanical competence of the vertebra. In particular, the lytic lesions most likely increase the risk of vertebral fracture (Kaneko et al., 2004). Even though different experimental and computational studies have clarified the effect of the metastasis on the whole bone structural behavior, their effect on the local mechanical properties is still unclear.

Finite element (FE) models are a powerful tool to predict the mechanical behavior of vertebrae for a certain subject (Crawford et al., 2003; Dall'Ara et al., 2012). In the past twenty years, FE models have been also used to study the effect of metastatic lesions on the vertebral mechanical properties. However, only a few models have been validated against experiments (Table 1). The comparison has been limited to the deformation of a few regions on the external surface of the vertebral body by using pointwise strain measurement obtained by strain gauges (Alkalay and Harrigan, 2016; Whyne et al., 2003), or to the apparent structural properties of the vertebral body (Stadelmann et al., 2020). Nevertheless, these approaches are not enough for understanding the ability of the FE models in predicting the heterogeneous local deformation driven by the complex and altered microstructure of bone tissue when affected by metastatic lesions. While these modelling approaches have great potential in predicting the bone strength in patients, the microstructure of the bone is not taken into account due to the low resolution of the input quantitative computed tomography (CT) images. Recently, micro computed tomography (microCT)-based FE models (microFE) have been developed to evaluate how bone microstructure and metastatic lesions affect the vertebral mechanical properties (Costa et al., 2020; Stadelmann et al., 2020). Despite the development and

* Corresponding author.
E-mail addresses: m.palanca@sheffield.ac.uk, marco.palanca@unibo.it (M. Palanca).

https://doi.org/10.1016/j.jmbbm.2021.104872
Received 10 March 2021; Received in revised form 21 September 2021; Accepted 30 September 2021
Available online 9 October 2021

usage of the microFE models, their ability of predicting the local mechanical properties within the vertebral body affected by lesions is still unknown.

The effect of the lytic lesions (artificial or real) on the vertebral body has been studied with experimental approaches (Alkalay, 2015; Hardisty et al., 2012; Palanca et al., 2018; Rezaei et al., 2021). In recent studies, vertebrae with induced lesions were mechanically tested through the intervertebral discs, and Digital Image Correlation (DIC) was used to characterize the surface strain pattern (Palanca et al., 2018; Rezaei et al., 2021). The results showed that the size of the lesion affects the surface strain distribution and larger lesions weaken the vertebra. Nevertheless, the DIC measurements are limited to the external surface of the bone and little is known about the effect of the lesions on the deformation of the internal structure. Digital Volume Correlation is the only available technique that can be used to evaluate the 3D displacement and strain fields inside the bone structure, enabling the validation of local model outputs. Measurements of the displacements can be performed with acceptable uncertainties, below the voxel size (Palanca et al., 2015). DVC displacement measurements have been previously used to validate the outputs of specimen specific microFE models and clinical CT-based FE models of different bone structures (Table 1). In particular, microFE models of vertebral body slices loaded under uniaxial compression showed excellent agreements with DVC data ($0.87 < R^2 < 0.99$) (Costa et al., 2017). Conversely, the predictions of local displacements from clinical CT-based FE models of vertebral bodies loaded through the intervertebral disc have shown a wide range of coefficient of determination when compared to local displacements measured with DVC ($0.06 < R^2 < 0.99$) (Hussein et al., 2018; (Jackman et al., 2016a); Wu and Morgan, 2020).

A protocol based on in situ mechanical testing, time-lapsed imaging and DVC was developed to evaluate differences in internal strain patterns between intact porcine vertebral bodies before and after the mechanical induction of focal lesions (Palanca et al., 2021). In all cases, the lesions lead to a highly inhomogeneous strain pattern if compared with intact vertebrae, with focal deformation in the closeness of the lesion. It remains to be investigated if linear microFE models can predict the local displacements, fundamental for the assessment of the effect of bone microstructure and lesions' properties on the mechanical properties of the bone. Despite differences in anatomy and loading conditions between porcine and human spines, porcine vertebrae have been used to define the testing protocol and explore the feasibility of new approaches thanks to their high inter-specimen similarity (Aziz et al., 2008; Costa et al., 2017; Danesi et al., 2016; Holsgrove et al., 2015; Palanca et al., 2018). However, the open growth plates and local gradients of density between hard and soft tissues in such regions may affect the local deformation in the tissue and potentially the predictions of the models.

The aim of the study was to validate the ability of linear microFE models in predicting internal displacements of porcine vertebrae tested through their intervertebral discs, either in intact conditions and with focal lesions by using DVC data. Moreover, the predictive ability of the microFE models that included different portions of the vertebra, with or without the growth plates, has been investigated.

2. Materials and methods

2.1. Specimens preparation

Five porcine spine segments, previously mechanically tested in (Palanca et al., 2021), were used in this study. Each spine segment consisted of three-vertebrae, (T8-10, 2x T10-T12, 2x T12-T14), in order to load the middle vertebra through the intervertebral discs. The anterior ligament, the fat tissues, the muscles around the spine segment and the posterior arch were removed from each spine segment. The cranial portion of the cranial vertebra and the caudal portion of the caudal vertebra were embedded in poly-methyl-methacrylate (4032, Technovit, Germany), in order to fix the specimens within a custom-made loading device. The specimens were initially tested in elastic regime (referred to as "intact", details in the Experimental data). Then, an artificial focal lesion was induced in each vertebral body using a pillar drill with an 8 mm diamond core tool. The semi-cylindrical lesions were induced in the middle frontal side (in specimens #1, #2 and #3) or left lateral side (in specimens #4 and #5) of the vertebral body, involving both cortical and trabecular bone. Lesion sizes ranged from 0.8% to 4.6% of the vertebral body. These different sizes and positions of the lesions were defined for challenging the models in predicting different distributions of local deformations induced by the lesions. These specimens (referred to as "lesioned") were tested again with the same procedure used for the intact ones.

Table 1
Summary of the validation studies performed on bone only using DVC data, where predictions for displacement fields are reported.

Study	Structure	Species	Load transmission	Image for DVC	Voxel size (um)	Image for FE	Element size (um)	Correlation between predicted and measured displacements
Zauel et al. (2006)	Trabecular bone	Human	Compression platens	MicroCT	35.0	MicroCT	35.0	$0.29 < R^2 < 0.97$
Chen et al. (2017)	Trabecular bone	Bovine/ Human	Compression platens	MicroCT	20.0–34.0	MicroCT	20.0–34.0	$0.97 < R^2 < 0.99$[a]
Costa et al. (2017)	Vertebral body	Porcine	Compression platens	MicroCT	39.0	MicroCT	39.0	$0.87 < R^2 < 0.99$
Oliviero et al. (2018)	Tibia	Mouse	Compression platens	MicroCT	10.4	MicroCT	10.4	$0.82 < R^2 < 0.99$
Oravec et al. (2019)	Vertebral body	Human	Compression platens	Digital tomosynthesis	280.0	MicroCT	40.0	$R^2 = 0.76$[b]
Jackman et al. (2016a)	Vertebral body	Human	Intervertebral discs	MicroCT	37.0	QCT	625.0	$0.06 < R^2 < 0.77$
Hussein et al. (2018)	Vertebral body	Human	Intervertebral discs	MicroCT	37.0	QCT	1240.0	$0.17 < R^2 < 0.84$[a]
Kusins et al. (2019)	Scapula	Human	Compression platens	MicroCT	33.5	QCT	625.0	$0.79 < R^2 < 1.00$[a]
Knowles et al. (2019)	Scapula	Human	Compression platens	MicroCT	33.5	QCT	625.0	$0.82 < R^2 < 1.00$
Wu and Morgan (2020)	Cuboid of trabecular bone within vertebral body	Human	Intervertebral discs	MicroCT	37.0	QCT	1240.0	$0.86 < R^2 < 0.99$[c]

[a] In the case where the boundary conditions were interpolated by the DVC.
[b] Only in z-direction.
[c] Orthotropic models, boundary conditions set in every external surface of the cuboid.

2.2. Experimental data

In situ experimental tests were performed within a microCT scanner (VivaCT80, Scanco, Switzerland) while imaging the specimen (Fig. 1). The following scanning parameters (Costa et al., 2020) were used: current 114 mA, voltage 70 kVp, integration time 300 ms, angular step 0.18°, total rotation 180°, power 8W, for a total of 92 min for each scan. An isotropic voxel size of 39 μm was obtained. The images were reconstructed using the software provided by the manufacturer that includes a beam hardening correction based on a phantom with 1200 mg HA/cm^3 density (Kazakia et al., 2008).

The specimens were axially compressed along the cranio-caudal (z) direction using a custom-made loading device, equipped with a 10 kN load cell (with a precision of 5 N) and a 20 mm Linear Variable Displacement Transducers (LVDT) (Ryan et al., 2020). The displacement was manually applied through a screw that does not allow spontaneous retrograde movement, with a ratchet wrench. Each specimen was preconditioned with 10 cycles between 50 and 300N, scanned under an axial pre-load of 50N, to avoid any movement during the scan, and scanned again under an axial load of 6500N, which is substantially lower than the typical failure load of porcine vertebrae, i.e. 17000 N (Allan et al., 1990). Tests were performed in displacement control until the nominal target load, after which the specimen underwent relaxation (fixed displacement, decreasing load). During relaxation, the specimen was allowed to settle, and the load was monitored. The scan started when the load reached a stabilization (plateau) to avoid moving artifacts, approximately 15 min after the application of the compression. The same procedure was repeated for each specimen, in both the intact and lesioned conditions. In case of failure, the loading procedure was immediately stopped without applying additional displacement, and the previously described procedure was applied. All microCT scans are available from the Figshare database, https://doi.org/10.15131/shef.data.16732441 or by contacting the corresponding author.

The displacement and strain fields within the bone were computed using a global DVC approach (BoneDVC, https://bonedvc.insigneo.org/dvc/) (Dall'Ara et al., 2017). The operating principles were extensively reported elsewhere (Dall'Ara et al., 2017, 2014; Palanca et al., 2021, 2015). Briefly, the microCT scans of the specimens were cropped to include only the middle vertebra. A parallelepiped grid with cubic cells, with side length equal to the nodal spacing (NS), was superimposed to the preloaded and loaded scans. The preloaded and loaded scans were elastically registered (Sheffield Image Registration Toolkit, ShIRT), solving the registration equations at the nodes of the grid, and obtaining the displacement field. The strains were then calculated by differentiating the displacement field using a FE software package (Mechanical APDL v19, ANSYS, USA) that was used also for the visualisation of the data and the comparison between experimental measurements and numerical prediction. Finally, all the cells of the grid with

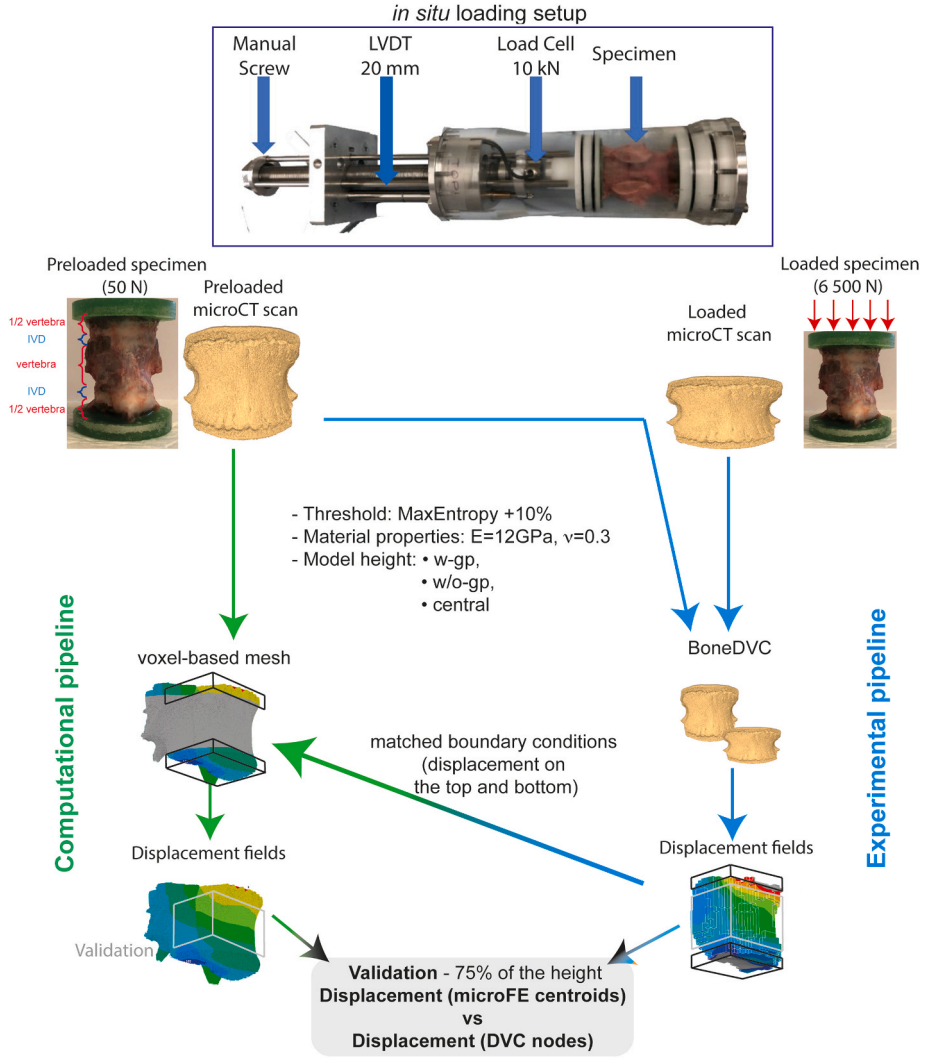

Fig. 1. In situ loading setup and workflow for the experimental and computational evaluation of the displacement. The same procedure was repeated for the intact and lesioned vertebrae.

all eight nodes outside of the vertebral body were removed.

Sensitivity analysis showed that a nodal spacing of 50 voxels was the optimal compromise between the measurement spatial resolution (equal to 1.95 mm) (Palanca et al., 2021) and the measurement uncertainty (displacement random error: 4.3 μm in x-direction, 3.1 μm in y-direction and 2.2 μm in z-direction; strain standard deviation of the error (SDER): 337 microstrain (Palanca et al., 2016)).

The displacement in right-left (x), antero-posterior (y) and cranio-caudal (z) direction, and the maximum and minimum principal strain were measured in all specimens at the nodes of the grid, both with and without the lesion.

2.3. microFE models

Voxel-based microFE models of the middle vertebra for each spine segments were created and used to predict the local displacements within the bone structure under loading (Chen et al., 2017; Costa et al., 2017). A 3D gaussian filter ($\sigma = 1.2$ and $k = 3$) was applied to the pre-loaded microCT images to reduce the high frequency noise. A single level threshold was chosen starting from the value based on the Max Entropy thresholding algorithm (Sahoo et al., 1988) (the inter-class entropy is maximized) and corrected by 10% to obtain binary images that best conserved the structure after visual inspection. Then, a connectivity filter was applied to remove voxels without any face connection.

The voxel-based mesh was created converting each bone voxel of the preloaded scan in an 8-nodes linear hexahedral element (Chen et al., 2017; Costa et al., 2017). Homogeneous and isotropic material properties, consisting in elastic modulus equal to 12 GPa and a Poisson's ratio of 0.3, were applied to the bone elements (Wolfram et al., 2010).

In order to understand the predictive ability of the microFE models in function of the considered region of interest, three different geometries were considered (Fig. 2):

- Including the growth plate and without the endplates, equal to the middle 80% of the total height of the vertebral body (later referred to as "w-gp"). Visual inspection of the remaining microCT cross-sections confirmed that the endplates were removed but the growth plates were still included in the image;
- Excluding the growth plate, equal to the middle 50% of the total height of the vertebral body (later referred as "w/o-gp"). Visual inspection of the remaining microCT cross-sections confirmed that the endplates and the growth plates were removed from the image;
- Considering only the middle region of the vertebra, where the lesion is created, equal to the 30% of the total height of the vertebral body (later referred to as "central").

Displacement boundary conditions, obtained from the DVC data, were imposed on the top and bottom single layer of the different models (Chen et al., 2017). The displacements measured in each node of these two layers were tri-linearly interpolated from the co-registered DVC grid to fit the microFE mesh and applied to the models. The Cartesian components of the displacement were computed in every node of the models, both with and without the lesion, for each specimen (Fig. 1). Finally, the values on the centroids of the elements were obtained as the average of the nodal values. All DVC and microFE results are available from the Figshare database, https://doi.org/10.15131/shef.data.16732441 or by contacting the corresponding author.

A high-performance computing cluster (ShARC) (64CPUs and maximum memory of 1.5 Tb), with Matlab 2017 (Mathworks, Inc, USA) and Mechanical APDL v19 (ANSYS, USA), was used to run the models.

2.4. Comparison between microFE and DVC

The DVC and microFE displacements were compared in the nodes of the DVC grid that were in the bone structure (by construction the nodes of the DVC grid are located in the centres of the microFE element). A point-by-point validation of predicted displacements against measured displacements was performed in the middle 75% portion of the model, in order to exclude those cranial and caudal nodes close to the application of the boundary conditions (Fig. 1).

No strain comparison between the DVC and microFE models was performed because the spatial resolution of the DVC measurements, required to obtain strain uncertainties low enough to be able to validate the models (Spatial resolution of 1.950 mm, SDER equal to 337 microstrain) (Palanca et al., 2021), was too low to perform a direct comparison of the strain values at the tissue level (i.e. within the trabeculae), which was predicted by the microFE models (spatial resolution equal to 0.039 mm).

2.5. Statistics

Validation was performed between the Cartesian components of the displacement measured by the DVC and predicted by the microFE models, for vertebrae with/without focal lesions and with/without growth plates. The degrees of agreement were reported in terms of

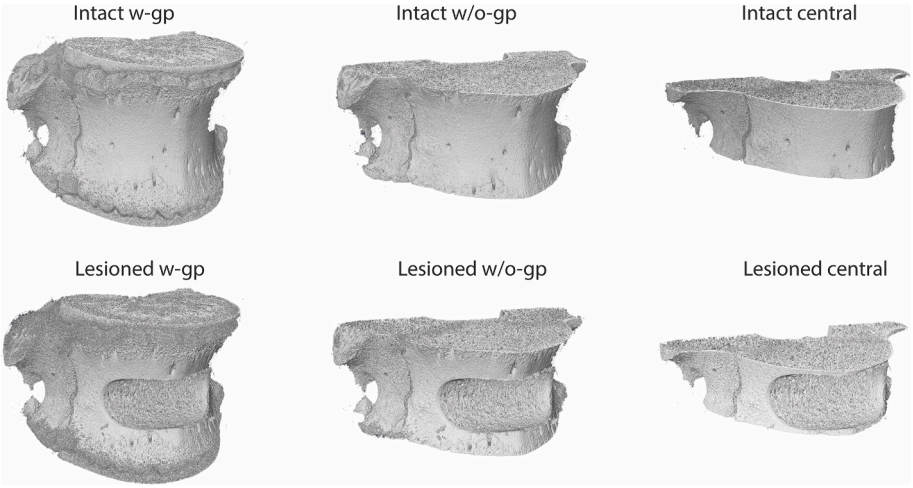

Fig. 2. Different microFE models prepared for each vertebra. On the top are the models of the intact vertebra with growth plates (w-gp), without the growth-plates (w/o-gp) and including only the central portion of the bone. On the bottom, the same three models were replicated on the vertebra after the creation of the focal lesion.

intercept, slope and coefficient of determination (R^2). To compare the correlation coefficients of intact and lesioned models, the correlation coefficients were transformed using the Fisher's r to z transformation, and z tests were performed.

The accuracy of the microFE to predict the displacement measured by the DVC was characterized reporting the following statistical parameters: root mean square error (RMSE); percentage RMSE (RMSE%), calculated as the ratio between the RMSE and the measured largest displacement in absolute value; and max error (MaxErr), calculated as the largest difference between the predicted and measured displacement among all nodes; the concordance correlation coefficient (CCC) between the DVC and the microFE results.

The statistics in the main text are reported without excluding potential outliers. For simplifying the comparison with the literature data are reported in the Supplementary Material after removal of the outliers, identified as observations with a Cook's distance larger than 5 times the average Cook's distance (Chen et al., 2017; Costa et al., 2017).

3. Results

The experimental tests were successfully performed loading each intact specimen at 6500N, without inducing any visible fracture. Indeed, only a few regions of the vertebral body close to the growth plates experienced deformation beyond the elastic regime (i.e. <-10000 microstrain). After the induction of the lesion, the specimen #2 and the specimen #3 failed at lower loads (3000N and 4500N, respectively). In these two cases, the experimental strain showed high strains localized close to the focal lesion, with magnitudes up to 80000 and 200000 microstrain, respectively.

The microFE models predicted well the displacements measured by the DVC in case of central models (central: R^2 from 0.69 to 1.00, $p < 0.0001$). Predictive accuracy lower than central models was found for models without growth plates (w/o-gp: R^2 from 0.56 to 1.00, $p < 0.0001$) and models including the growth plates (w-gp: R^2 from 0.02 to 0.99, $p < 0.0001$ except for specimen #5 intact in y direction, p-value = 0.1261) (Fig. 3). Similar trends, with better predictions in central models than in models including the growth plates, were observed for both intact and lesioned models (Fig. 4 and Fig. 5).

The lift-up of the displacements in z-direction of Specimen 2 and Specimen 3 was the consequence of the failure around the lesion, that caused the movement of the bottom part toward the top.

In those cases where the growth plates were included, the intact models predicted less well the experimental displacements compared to those for the lesioned vertebrae (Figs. 3 and 4). In most cases, the correlation coefficients were significantly different (Table S1). A local analysis within the volume of the vertebra showed that larger percentage errors were localized in the regions of the growth plates (Fig. 6). The correlation drastically improved just with the reduction of the model height excluding the growth plates (see Supplementary Materials: Table S1 and Table S2).

The results for correlation analyses after the removal of the outliers are reported in Table S3-Table S5. Minor differences can be observed between the results before and after the removal of the outliers.

By contrast, considering the central models, more accurate predictions of the displacements were observed in the models of the intact vertebrae with respect to the one based on the geometry of the lesioned vertebrae (Table 2, Fig. 6). Except four cases (i.e. specimen #1 in x direction, specimen #2 in y and z directions, and specimen #4 in z direction), the correlation coefficients were significantly different, with better performance in case of intact vertebrae. Specimens that deformed beyond yield when lesioned (specimens #2 and #3) showed the largest RMSE and Max Error, indicating poorer agreements between measured and predicted displacements. In particular, the Max Error for Specimen #3 was 2–9 times larger than the voxel size.

No systematic preferential directions were observed in the different cases.

4. Discussion

The aim of this study was to understand the ability of microFE models of porcine vertebral bodies loaded through the intervertebral discs, with and without the induction of focal lesions, in predicting the local displacements against experimental measurements performed with DVC.

The central vertebra of each spine segment was loaded under complex loading conditions through the intervertebral discs (Hussein et al., 2013). This scenario represents a more physiological loading condition since the load is heterogeneously distributed through the endplates

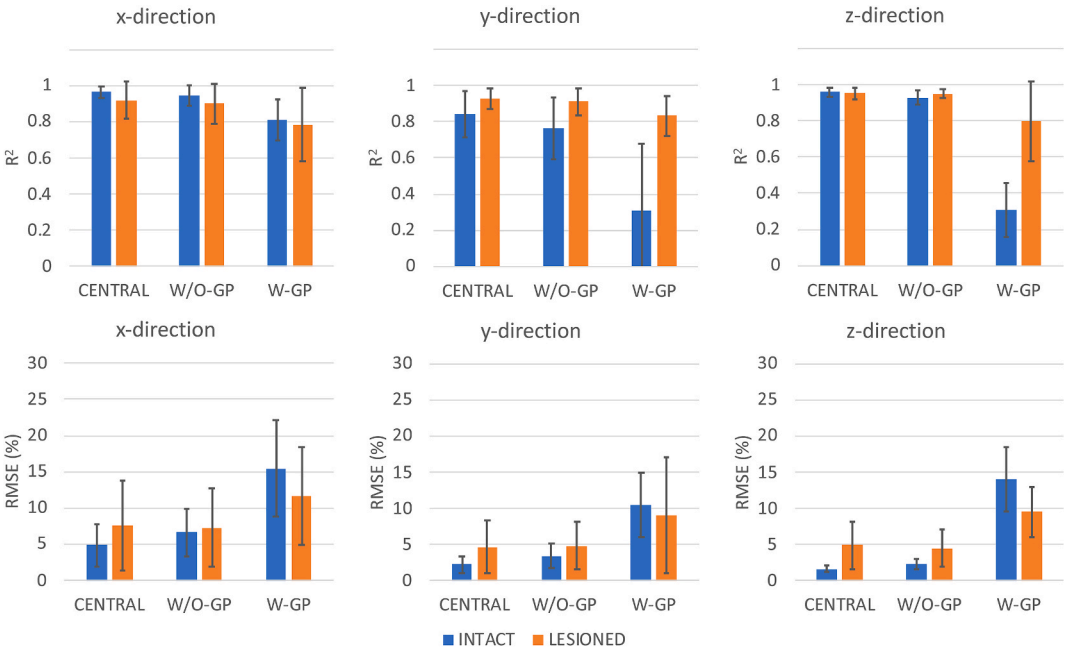

Fig. 3. Coefficients of determination (R^2, in the first row) and percentage root mean square errors (RMSE(%), in the second row) over the sample for the different models. Data are reported as average, errors bars represent standard deviations among the five specimens.

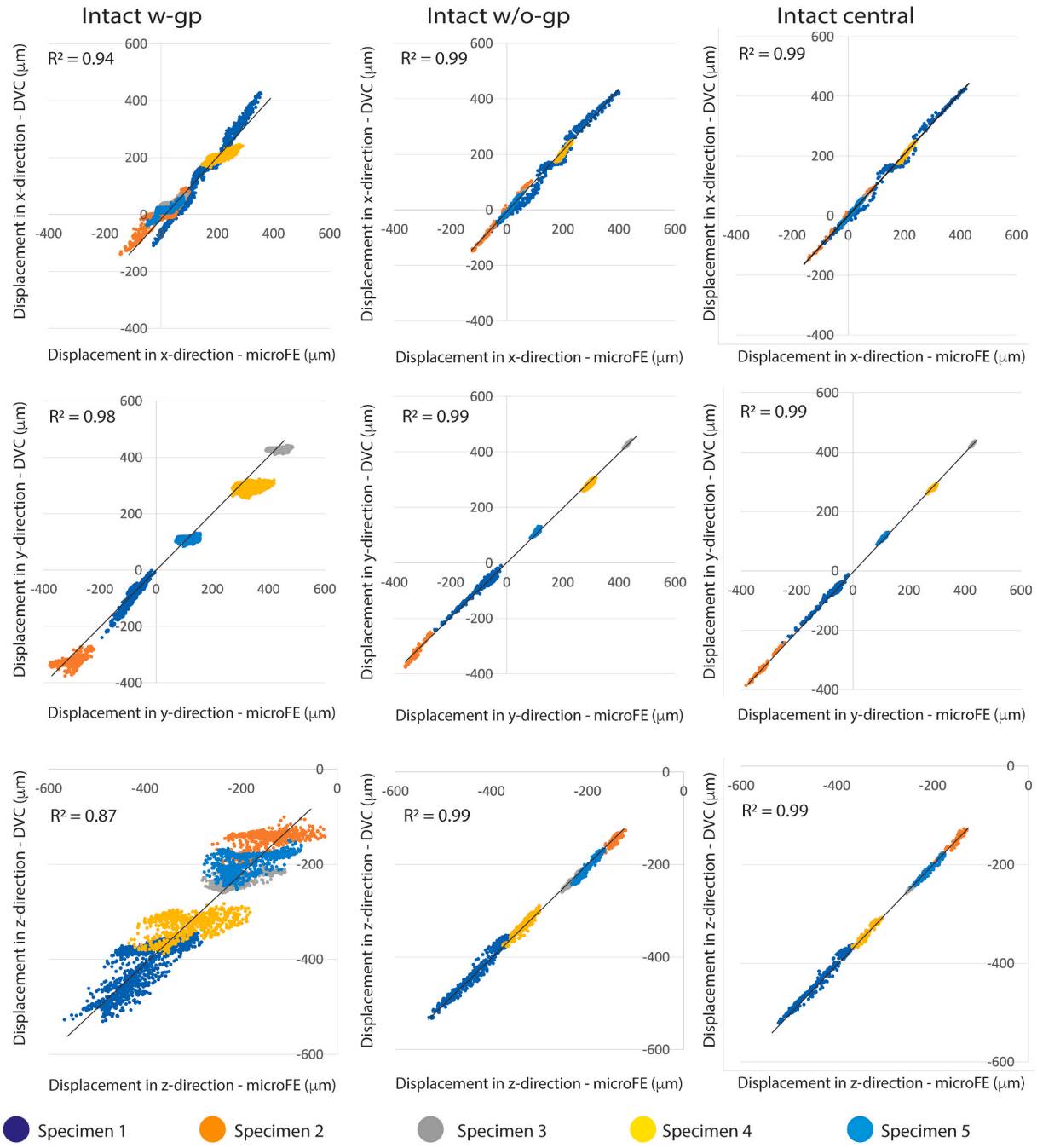

Fig. 4. Correlation analysis between the displacement measured by the DVC (y-axis) and the displacement predicted by the microFE (x-axis) for models of intact vertebrae. Each colour represents a different specimen. For each plot, the coefficients of determination aggregated over the entire sample are reported. The aggregated regression lines are reported in black, the 1:1 relationships are reported as red dashed lines. (For interpretation of the references to colour in this figure legend, the reader is referred to the Web version of this article.)

rather than homogeneously applied through embedding caps of PMMA or cement (Costa et al., 2017). In particular, loading the vertebral bodies through the discs induced larger transverse displacements and more heterogeneous deformation in the vertebral body. The validation analysis showed that the linear microFE models were able to predict the displacement fields in the elastic regime within the vertebral body, both with and without focal lesions. The better results were observed for central models of vertebrae without any lesions. As observed from results, in this case only a limited number of regions of the vertebra experienced experimental strains beyond the conventionally accepted bone elastic regime (7300 microstrain for maximum principal strain and −10400 microstrain for minimum principal strain (Bayraktar et al., 2004)). In fact, the level of agreement between measured and predicted displacement was comparable with the work of Costa et al. (2017), which validated models of porcine vertebral bodies directly embedded in orthopaedic cement. Thus, the small differences between the correlation of measured and predicted displacements ($0.65 < R^2 < 1.00$ in this study versus $0.87 < R^2 < 0.99$ in Costa et al.) calculated in the two studies could be explained by the different boundary conditions in experiments and models. Larger variability was obtained in the studies by (Hussein et al., 2018; Jackman et al., 2016a,b) (R^2 from 0.06 to 0.84) in which human vertebrae were tested. However, it must be taken into account that in those studies different modelling and DVC approaches were used. The presence of focal lesions, in addition to the loading

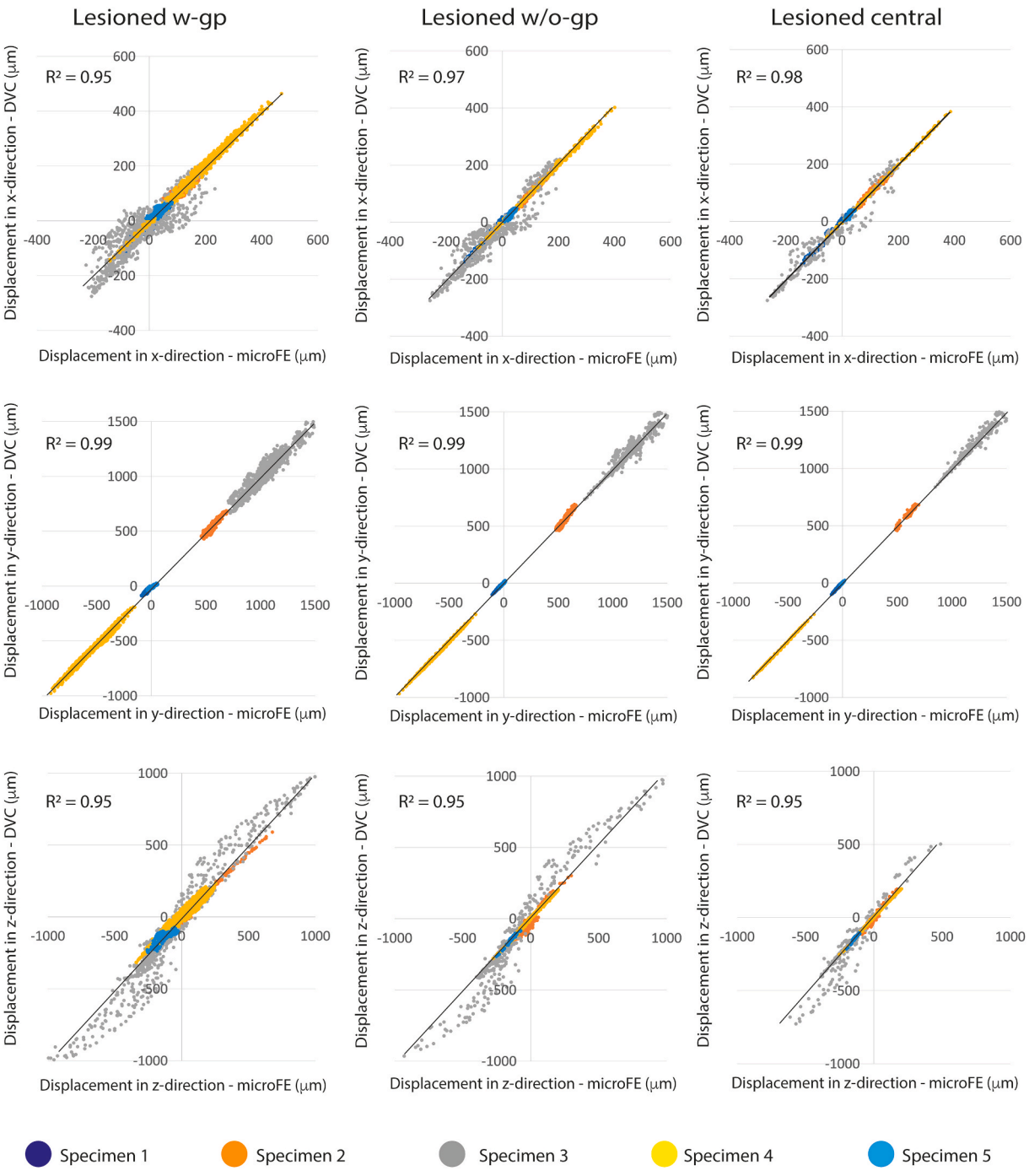

Fig. 5. Correlation analysis between the displacement measured by the DVC (y-axis) and the displacement predicted by the μFE (x-axis) for models of vertebrae with induced lesion. Each colour represents a different specimen. For each plot, the coefficients of determination aggregated over the entire sample are reported. The aggregated regression lines are reported in black, the 1:1 relationships are reported as red dashed lines. (For interpretation of the references to colour in this figure legend, the reader is referred to the Web version of this article.)

through intervertebral discs, could induce high localized damage in the specimens, depending on the size and position of the lesions. This reduced the model ability of predicting local displacements, although it remained still excellent in most cases. In fact, when the strength of the specimens was too much reduced by the lesions (specimens #2 and #3), the model predicted beyond the 74% of the variance but with errors larger than 6 voxels (approximately 0.25 mm). These high errors were localized close to the lesions, where the bone tissue yielded. Linear microFE models cannot correctly predict the local bone post-yield and failure behavior. In fact, in these cases a nonlinear model including material damage (Stipsitz et al., 2021) is preferred to identify the failed regions. However, before its application to study the deformation of the vertebral body proper model validation should be performed and the efficiency of the models should be increased. Nevertheless, the linear microFE models are useful to evaluate the effect of different lesions before the yield (e.g. on the stiffness, displacements, strain distributions) that can be used to extrapolate the structural failure load as shown for different bone structures (Oliviero et al., 2021; Pahr et al., 2012; Pistoia et al., 2002). The results of the validation study revealed the importance of the selection of the modelled region of interest within the vertebral

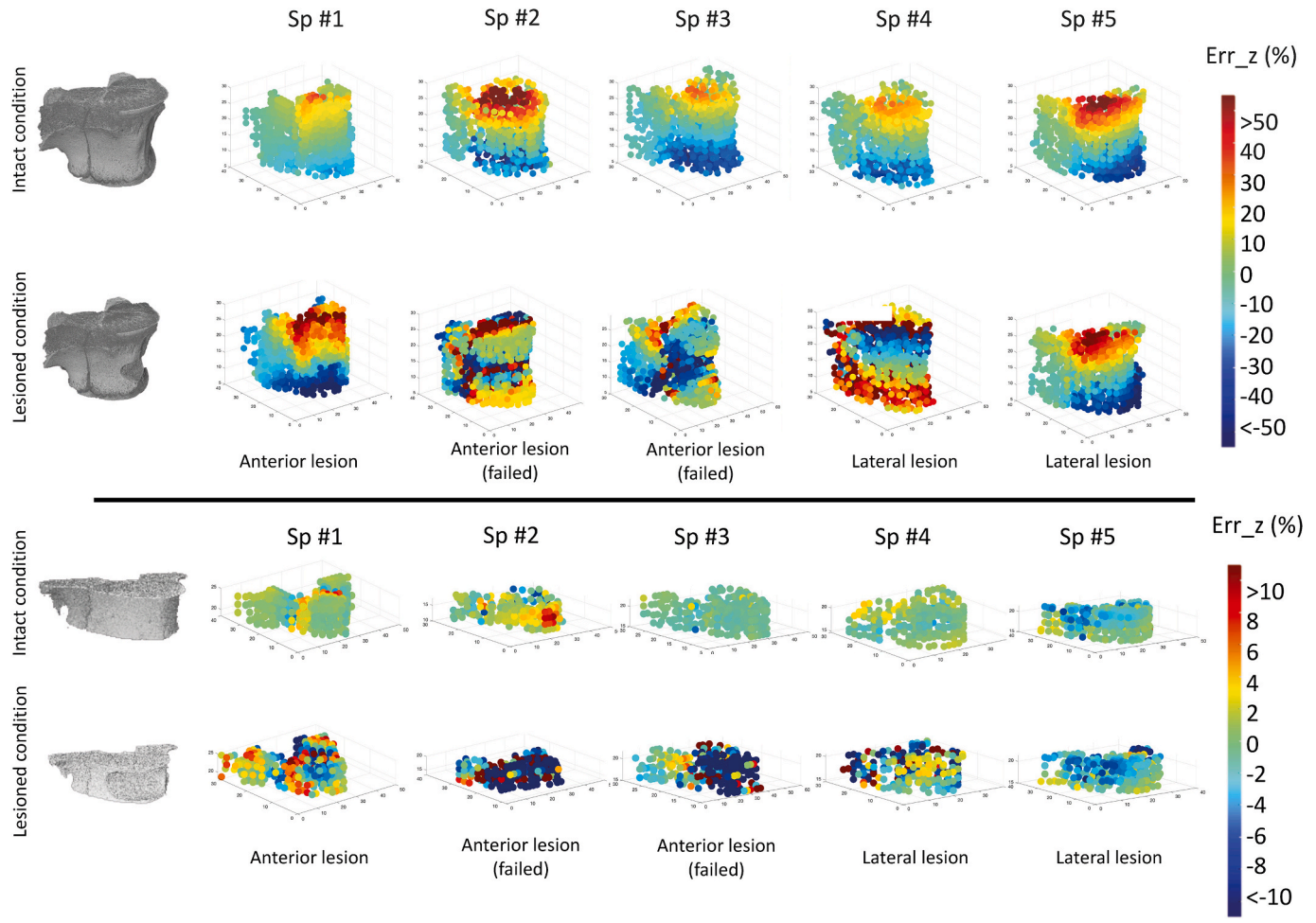

Fig. 6. Error distributions evaluated as the difference between the microFE predicted and DVC measured axial displacement (z-axis), divided by the measured displacement. Erros are reported for the intact and lesioned models with growth plates (top), and intact and lesioned central models (bottom). On the left, 3D examples of intact and lesioned vertebrae are reported.

body. Indeed, while using porcine vertebrae represents an excellent strategy to standardize the protocol and mitigate the inter-specimens variability, the outcomes could be largely affected by the growth plates that are still open in juvenile porcine bones (Raimann et al., 2017). These regions could experience permanent deformation and the DVC performance, in terms of accuracy and precision, could be negatively affected by the large deformations of the soft tissues within the growth plates, which are not visible in the microCT images. In fact, in the intact specimens the growth plates were the regions with the largest displacement errors (Fig. 6). In the lesioned specimens, instead, errors in the growth plates regions were smaller than in the case of intact specimens, and large displacement errors were localized close to the lesion. These contrasting behaviors could be due to a residual deformation of the soft tissues within the growth plates caused during the first test with intact specimens (Cohen et al., 1994; Hardisty et al., 2010), which reduces the effect of material nonlinearities on the deformation of the structure.

The good correlations between measured and predicted displacements, suggest that the microFE modelling approach can be used to explore the effect of the metastatic features (i.e. size, shape and position) on the competence of the vertebral body. Nevertheless, it should be stressed that the application of the models for answering clinical or biological questions should be performed on human specimens with a bone maturity coherent with the studied disease.

This study suffers from some limitations. Firstly, porcine vertebrae with artificial focal lesion were used instead of human vertebrae with actual metastasis. This choice was made just for defining the whole experimental and computational pipelines. During the experimental tests, a uniaxial load cell was used to measure the applied axial load. Considering that the vertebrae were loaded through the intervertebral discs, substantial transverse forces were probably present during the load. Due to this simplification the stiffness of the bone could not be properly estimated and compared with the microFE models. While a six-components load cell would have provided the required outputs, the limited space in the microCT scanner did not allow re-design the testing device in order to accommodate the larger sensor. Secondly, the validation of the model outputs was focused on the displacements. This choice was driven by the compromise between spatial resolution and precision that has to be accepted when performing DVC measurements of large specimens (Dall'Ara et al., 2017). Nevertheless, the validation of the estimated local strain values from microFE models would give more credibility to multiscale models developed to predict bone remodelling over time (Christen et al., 2014). However, in order to validate the model at the trabecular level, more accurate DVC measurements, which could be based on high resolution input images (e.g. from Synchrotron radiation microCT (Palanca et al., 2017)), are needed. Still, such resolution cannot be obtained yet for large bone structures as the whole vertebral body. Finally, simple homogeneous isotropic linear microFE models were used. While it is accepted that bone is locally heterogeneous and its properties depend on the local tissue mineral density (Gross et al., 2012) little is known about the variability in local mineralization in vertebrae with realistic metastases or around the regions of

Table 2
Linear regression analyses for each direction in central models of intact and lesioned vertebrae.

Specimen	Direction	Points	Slope	Intercept [um]	R^2	RMSE [um]	RMSE%	MaxErr [um]	CCC	p-value (z-test)
# 1	X – intact	388	1.06	−8.06	0.99	16.94	3.99	50	12	1.00
Anteriorly lesioned	X - lesioned	358	1.02	1.25	0.99	6.64	4.30	25	16	
	Y - intact	388	0.94	−5.55	0.98	7.55	3.11	24	10	<0.001
	Y - lesioned	358	0.98	2.43	0.94	6.29	5.89	30	28	
	Z - intact	388	1.03	12.93	0.97	7.97	1.53	30	6	<0.001
	Z - lesioned	358	0.99	−0.91	0.92	4.39	3.13	22	16	
# 2	X – intact	227	1.05	2.90	0.99	6.48	4.43	33	22	<0.001
Anteriorly lesioned	X - lesioned	231	0.98	−0.47	0.95	7.79	4.03	24	13	
	Y - intact	227	1.09	26.35	0.96	6.08	1.58	28	7	1.00
	Y - lesioned	231	1.10	−61.30	0.95	18.16	2.51	60	8	
	Z - intact	227	1.03	5.71	0.95	4.36	2.20	21	11	0.343
	Z - lesioned	231	1.11	1.38	0.94	14.97	7.71	50	26	
# 3	X – intact	288	1.04	0.05	0.99	2.71	3.76	8	11	<0.001
Anteriorly lesioned	X - lesioned	261	0.94	−10.54	0.93	38.53	14.00	146	53	
	Y - intact	288	0.99	4.01	0.84	1.99	0.45	7	2	<0.001
	Y - lesioned	261	0.94	77.63	0.92	48.87	3.18	230	15	
	Z - intact	288	1.00	−1.73	0.98	3.11	1.20	12	5	<0.001
	Z - lesioned	261	1.13	6.88	0.93	69.79	9.20	247	33	
# 4	X – intact	261	1.19	−38.45	0.92	5.76	2.23	19	7	<0.001
Laterally lesioned	X - lesioned	213	1.00	−2.11	1.00	3.89	1.01	10	3	
	Y - intact	261	0.77	58.05	0.69	7.91	2.68	19	6	<0.001
	Y - lesioned	213	0.99	−15.43	1.00	10.53	1.27	21	3	
	Z - intact	261	1.03	8.70	0.92	5.26	1.42	16	4	<0.001
	Z - lesioned	213	1.01	−0.43	1.00	5.00	1.98	18	7	
# 5	X – intact	302	1.08	−0.88	0.94	5.78	9.91	16	28	<0.001
Laterally lesioned	X - lesioned	278	1.03	−2.44	0.74	5.99	14.51	21	50	
	Y - intact	302	0.87	16.29	0.74	4.45	3.32	13	10	<0.001
	Y - lesioned	278	1.09	2.45	0.83	4.25	10.47	21	53	
	Z - intact	302	1.01	0.19	0.97	4.76	1.94	17	7	1.00
	Z - lesioned	278	1.12	11.88	0.97	6.24	2.43	27	11	

the growth plate in the tested porcine vertebrae. Heterogeneous models based on imaging modalities that enable an accurate representation of the local mineralization (e.g. calibrated Synchrotron microCT imaging) have the potential of improving the predictions of local bone deformation and could be tested in future studies, especially for human bones with real metastases.

5. Conclusion

This study confirmed the optimal ability of homogeneous isotropic linear microFE models in predicting the local displacements in vertebral bodies induced by complex loading. The findings showed that despite the lesions induce non-homogeneous displacement/strain distributions, the performance of the microFE models is not compromized when the specimens are loaded in an elastic regime. By contrast, regions like the growth plates, where non-linear behavior could be expected, should be excluded. While these simplified models can be used to predict complex deformation fields in the elastic regime, the results on a few specimens tested beyond yield suggest that more complex non-linear models should be developed to predict the deformation in regions with high strain. Nevertheless, the microFE approach applied to a large database of microCT images of the human vertebra, has great potential of elucidating the effect of lesion's properties (e.g. size, shape, location) on the vertebral mechanical properties.

CRediT authorship contribution statement

Marco Palanca: Conceptualization, Investigation, Data curation, Writing – original draft, Project administration, Funding acquisition. **Sara Oliviero:** Conceptualization, Methodology, Writing – review & editing. **Enrico Dall'Ara:** Conceptualization, Funding acquisition, Resources, Writing – review & editing, Supervision.

Declaration of competing interest

The authors declare that they have no known competing financial interests or personal relationships that could have appeared to influence the work reported in this paper.

Acknowledgements

The authors would like to thank Ms Giulia De Donno for the help during the experimental tests, Mr Simon Rawson for the jig repair and Ms Giulia Cavazzoni for proof-reading the manuscript.

The study was partially supported by Marie Skłodowska-Curie Individual Fellowship (MetaSpine, MSCA–IF–EF-ST, 832430/2018), by the Engineering and Physical Sciences Research Council (EPSRC) Frontier Multisim Grant (EP/K03877X/1 and EP/S032940/1), by the AOSpine Discovery and Innovation Awards (AOSDIA_2019_063_TUM_Palanca). The SkeletAl laboratory is acknowledged for the access to the imaging facilities.

The funders had no role in study design, data collection or analysis, decision to publish, or preparation of the manuscript.

Appendix A. Supplementary data

Supplementary data to this article can be found online at https://doi.org/10.1016/j.jmbbm.2021.104872.

Declaration of competing interest

The authors have no conflict of interest to declare.

References

Alkalay, R.N., 2015. Effet of the metastatic defect on the structural responde and failure process of human vertebrae: an experimental study. Clin. BioMech. 30, 121–128.

Alkalay, R.N., Harrigan, T.P., 2016. Mechanical assessment of the effects of metastatic lytic defect on the structural response of human thoracolumbar spine: effect OF critical lytic defect. J. Orthop. Res. 34, 1808–1819. https://doi.org/10.1002/jor.23154.

Allan, D.G., Russell, G.G., Moreau, M.J., Raso, V.J., Budney, D., 1990. Vertebral end-plate failure in porcine-and bovine models of spinal fracture instrumentation. J. Orthop. Res. 8, 154–156. https://doi.org/10.1002/jor.1100080121.

Aziz, H.N., Galbusera, F., Bellini, C.M., Mineo, G.V., Addis, A., Pietrabissa, R., Brayda-Bruno, M., 2008. Porcine models in spinal Research: calibration and comparative finite element analysis of various configurations during flexion–extension. Comp. Med. 58, 6.

Bayraktar, H.H., Morgan, E.F., Niebur, G.L., Morris, G.E., Wong, E.K., Keaveny, T.M., 2004. Comparison of the elastic and yield properties of human femoral trabecular and cortical bone tissue. J. Biomech. 37, 27–35. https://doi.org/10.1016/S0021-9290(03)00257-4.

Chen, Y., Dall'Ara, E., Sales, E., Manda, K., Wallace, R., Pankaj, P., Viceconti, M., 2017. Micro-CT based finite element models of cancellous bone predict accurately displacement once the boundary condition is well replicated: a validation study. Journal of the Mechanical Behavior of Biomedical Materials 65, 644–651. https://doi.org/10.1016/j.jmbbm.2016.09.014.

Christen, P., Ito, K., Ellouz, R., Boutroy, S., Sornay-Rendu, E., Chapurlat, R.D., van Rietbergen, B., 2014. Bone remodelling in humans is load-driven but not lazy. Nat. Commun. 5, 4855. https://doi.org/10.1038/ncomms5855.

Cohen, B., Chorney, G.S., Phillips, D.P., Dick, H.M., Mow, V.C., 1994. Compressive stress-relaxation behavior of bovine growth plate may be described by the nonlinear biphasic theory. J. Orthop. Res. 12, 804–813. https://doi.org/10.1002/jor.1100120608.

Costa, M.C., Campello, L.B.B., Ryan, M., Rochester, J., Viceconti, M., Dall'Ara, E., 2020. Effect of size and location of simulated lytic lesions on the structural properties of human vertebral bodies, a micro-finite element study. Bone Reports 12, 100257. https://doi.org/10.1016/j.bonr.2020.100257.

Costa, M.C., Tozzi, G., Cristofolini, L., Danesi, V., Viceconti, M., Dall'Ara, E., 2017. Micro Finite Element models of the vertebral body: validation of local displacement predictions. PLoS One 12, e0180151. https://doi.org/10.1371/journal.pone.0180151.

Crawford, R.P., Cann, C.E., Keaveny, T.M., 2003. Finite element models predict in vitro vertebral body compressive strength better than quantitative computed tomography. Bone 33, 744–750. https://doi.org/10.1016/S8756-3282(03)00210-2.

Dall'Ara, E., Barber, D., Viceconti, M., 2014. About the inevitable compromise between spatial resolution and accuracy of strain measurement for bone tissue: a 3D zero-strain study. J. Biomech. 47, 2956–2963. https://doi.org/10.1016/j.jbiomech.2014.07.019.

Dall'Ara, E., Pahr, D., Varga, P., Kainberger, F., Zysset, P., 2012. QCT-based finite element models predict human vertebral strength in vitro significantly better than simulated DEXA. Osteoporos. Int. 23, 563–572. https://doi.org/10.1007/s00198-011-1568-3.

Dall'Ara, E., Peña-Fernández, M., Palanca, M., Giorgi, M., Cristofolini, L., Tozzi, G., 2017. Precision of digital volume correlation approaches for strain analysis in bone imaged with micro-computed tomography at different dimensional levels. Front. Mater. 4, 31. https://doi.org/10.3389/fmats.2017.00031.

Danesi, V., Tozzi, G., Cristofolini, L., 2016. Application of digital volume correlation to study the efficacy of prophylactic vertebral augmentation. Clin. BioMech. 39, 14–24. https://doi.org/10.1016/j.clinbiomech.2016.07.010.

Gross, T., Pahr, D.H., Peyrin, F., Zysset, P.K., 2012. Mineral heterogeneity has a minor influence on the apparent elastic properties of human cancellous bone: a SRμCT-based finite element study. Comput. Methods Biomech. Biomed. Eng. 15, 1137–1144. https://doi.org/10.1080/10255842.2011.581236.

Hardisty, M.R., Akens, M., Yee, A.J., Whyne, C.M., 2010. Image registration demonstrates the growth plate has a variable affect on vertebral strain. Ann. Biomed. Eng. 38, 2948–2955. https://doi.org/10.1007/s10439-010-0052-0.

Hardisty, M.R., Akens, M.K., Hojjat, S.-P., Yee, A., Whyne, C.M., 2012. Quantification of the effect of osteolytic metastases on bone strain within whole vertebrae using image registration: effect OF osteolytic metastases ON bone strain. J. Orthop. Res. 30, 1032–1039. https://doi.org/10.1002/jor.22045.

Holsgrove, T.P., Cazzola, D., Preatoni, E., Trewartha, G., Miles, A.W., Gill, H.S., Gheduzzi, S., 2015. An investigation into axial impacts of the cervical spine using digital image correlation. Spine J. 15, 1856–1863. https://doi.org/10.1016/j.spinee.2015.04.005.

Hussein, A.I., Louzeiro, D.T., Unnikrishnan, G.U., Morgan, E.F., 2018. Differences in trabecular microarchitecture and simplified boundary conditions limit the accuracy of quantitative computed tomography-based finite element models of vertebral failure. J. Biomech. Eng. 140, 021004 https://doi.org/10.1115/1.4038609.

Hussein, A.I., Mason, Z.D., Morgan, E.F., 2013. Presence of intervertebral discs alters observed stiffness and failure mechanisms in the vertebra. J. Biomech. 46, 1683–1688. https://doi.org/10.1016/j.jbiomech.2013.04.004.

Jackman, Timothy M., DelMonaco, A.M., Morgan, E.F., 2016a. Accuracy of finite element analyses of CT scans in predictions of vertebral failure patterns under axial compression and anterior flexion. J. Biomech. 49, 267–275. https://doi.org/10.1016/j.jbiomech.2015.12.004.

Jackman, Timothy M., Hussein, A.I., Curtiss, C., Fein, P.M., Camp, A., De Barros, L., Morgan, E.F., 2016b. Quantitative, 3D visualization of the initiation and progression of vertebral fractures under compression and anterior flexion: visualization OF initiation and progression OF vertebral fracture. J. Bone Miner. Res. 31, 777–788. https://doi.org/10.1002/jbmr.2749.

Kaneko, T.S., Bell, J.S., Pejcic, M.R., Tehranzadeh, J., Keyak, J.H., 2004. Mechanical properties, density and quantitative CT scan data of trabecular bone with and without metastases. J. Biomech. 37, 523–530. https://doi.org/10.1016/j.jbiomech.2003.08.010.

Kazakia, G.J., Burghardt, A.J., Cheung, S., Majumdar, S., 2008. Assessment of bone tissue mineralization by conventional x-ray microcomputed tomography: comparison with synchrotron radiation microcomputed tomography and ash measurements: assessment of bone tissue mineralization by microcomputed tomography. Med. Phys. 35, 3170–3179. https://doi.org/10.1118/1.2924210.

Knowles, N.K., Kusins, J., Faieghi, M., Ryan, M., Dall'Ara, E., Ferreira, L.M., 2019. Material mapping of QCT-derived scapular models: a comparison with micro-CT loaded specimens using digital volume correlation. Ann. Biomed. Eng. 47, 2188–2198. https://doi.org/10.1007/s10439-019-02312-2.

Kusins, J., Knowles, N., Ryan, M., Dall'Ara, E., Ferreira, L., 2019. Performance of QCT-Derived scapula finite element models in predicting local displacements using digital volume correlation. Journal of the Mechanical Behavior of Biomedical Materials 97, 339–345. https://doi.org/10.1016/j.jmbbm.2019.05.021.

Laufer, I., Rubin, D.G., Lis, E., Cox, B.W., Stubblefield, M.D., Yamada, Y., Bilsky, M.H., 2013. The NOMS framework: approach to the treatment of spinal metastatic tumors. Oncol. 18, 744–751. https://doi.org/10.1634/theoncologist.2012-0293.

Oliviero, S., Giorgi, M., Dall'Ara, E., 2018. Validation of finite element models of the mouse tibia using digital volume correlation. Journal of the Mechanical Behavior of Biomedical Materials 86, 172–184. https://doi.org/10.1016/j.jmbbm.2018.06.022.

Oliviero, S., Roberts, M., Owen, R., Reilly, G.C., Bellantuono, I., Dall'Ara, E., 2021. Non-invasive prediction of the mouse tibia mechanical properties from microCT images: comparison between different finite element models. Biomech. Model. Mechanobiol. 20, 941–955. https://doi.org/10.1007/s10237-021-01422-y.

Oravec, D., Flynn, M.J., Zauel, R., Rao, S., Yeni, Y.N., 2019. Digital tomosynthesis based digital volume correlation: a clinically viable noninvasive method for direct measurement of intravertebral displacements using images of the human spine under physiological load. Med. Phys. 46, 4553–4562. https://doi.org/10.1002/mp.13750.

Pahr, D.H., Dall'Ara, E., Varga, P., Zysset, P.K., 2012. HR-pQCT-based homogenised finite element models provide quantitative predictions of experimental vertebral body stiffness and strength with the same accuracy as μFE models. Comput. Methods Biomech. Biomed. Eng. 15, 711–720. https://doi.org/10.1080/10255842.2011.556627.

Palanca, M., Barbanti-Bròdano, G., Cristofolini, L., 2018. The size of simulated lytic metastases affects the strain distribution on the anterior surface of the vertebra. J. Biomech. Eng. 140, 111005. https://doi.org/10.1115/1.4040587.

Palanca, M., Bodey, A.J., Giorgi, M., Viceconti, M., Lacroix, D., Cristofolini, L., Dall'Ara, E., 2017. Local displacement and strain uncertainties in different bone types by digital volume correlation of synchrotron microtomograms. J. Biomech. 58, 27–36. https://doi.org/10.1016/j.jbiomech.2017.04.007.

Palanca, M., Cristofolini, L., Dall'Ara, E., Curto, M., Innocente, F., Danesi, V., Tozzi, G., 2016. Digital volume correlation can be used to estimate local strains in natural and augmented vertebrae: An organ-level study. J. Biomech. 49, 3882–3890. https://doi.org/10.1016/j.jbiomech.2016.10.018.

Palanca, M., De Donno, G., Dall'Ara, E., 2021. A novel approach to evaluate the effects of artificial bone focal lesion on the three-dimensional strain distributions within the vertebral body. PLoS One 16, e0251873. https://doi.org/10.1371/journal.pone.0251873.

Palanca, M., Tozzi, G., Cristofolini, L., Viceconti, M., Dall'Ara, E., 2015. Three-Dimensional local measurements of bone strain and displacement: comparison of three digital volume correlation approaches. J. Biomech. Eng. 137, 071006 https://doi.org/10.1115/1.4030174.

Pistoia, W., van Rietbergen, B., Lochmüller, E.-M., Lill, C.A., Eckstein, F., Rüegsegger, P., 2002. Estimation of distal radius failure load with micro-finite element analysis models based on three-dimensional peripheral quantitative computed tomography images. Bone 30, 842–848. https://doi.org/10.1016/S8756-3282(02)00736-6.

Raimann, A., Javanmardi, A., Egerbacher, M., Haeusler, G., 2017. A journey through growth plates: tracking differences in morphology and regulation between the spine and the long bones in a pig model. Spine J. 17, 1674–1684. https://doi.org/10.1016/j.spinee.2017.06.001.

Rezaei, A., Tilton, M., Giambini, H., Li, Y., Hooke, A., Miller, A., Yaszemski, L., Lu, L., 2021. Three-dimensional surface strain analyses of simulated defect and augmented spine segments: a biomechanical cadaveric study. J Mech Behav Biomed Mater 119, 104559.

Roodman, D., 2004. Mechanisms of bone metastasis. N. Engl. J. Med. 10.

Ryan, M.K., Oliviero, S., Costa, M.C., Wilkinson, J.M., Dall'Ara, E., 2020. Heterogeneous strain distribution in the subchondral bone of human osteoarthritic femoral heads, measured with digital volume correlation. Materials 13, 4619. https://doi.org/10.3390/ma13204619.

Sahoo, P.K., Soltani, S., Wong, A.K.C., 1988. A survey of thresholding techniques. Comput. Vis. Graph Image Process 41, 233–260. https://doi.org/10.1016/0734-189X(88)90022-9.

Stadelmann, M.A., Schenk, D.E., Maquer, G., Lenherr, C., Buck, F.M., Bosshardt, D.D., Hoppe, S., Theumann, N., Alkalay, R.N., Zysset, P.K., 2020. Conventional finite element models estimate the strength of metastatic human vertebrae despite alterations of the bone's tissue and structure. Bone 141, 115598. https://doi.org/10.1016/j.bone.2020.115598.

Stipsitz, M., Zysset, P.K., Pahr, D.H., 2021. Prediction of the inelastic behaviour of radius segments: damage-based nonlinear micro finite element simulation vs Pistoia criterion. J. Biomech. 116, 110205. https://doi.org/10.1016/j.jbiomech.2020.110205.

Whyne, C.M., Hu, S.S., Lotz, J.C., 2003. Burst fracture in the metastatically involved spine: development, validation, and parametric analysis of a three-dimensional poroelastic finite-element model. Spine 28, 652–660. https://doi.org/10.1097/01.BRS.0000051910.97211.BA.

Wolfram, U., Wilke, H.-J., Zysset, P.K., 2010. Rehydration of vertebral trabecular bone: influences on its anisotropy, its stiffness and the indentation work with a view to age, gender and vertebral level. Bone 46, 348–354. https://doi.org/10.1016/j.bone.2009.09.035.

Wu, Y., Morgan, E.F., 2020. Effect of fabric on the accuracy of computed tomography-based finite element analyses of the vertebra. Biomech. Model. Mechanobiol. 19, 505–517. https://doi.org/10.1007/s10237-019-01225-2.

Zauel, R., Yeni, Y.N., Bay, B.K., Dong, X.N., Fyhrie, D.P., 2006. Comparison of the linear finite element prediction of defomration and strain of human cancellous bone to 3D digital volume correlation measurements. J. Biomech. Eng. 128, 1–6.